

A Cubic 3d–4f Structure with Only Ferromagnetic Gd–Mn Interactions**

Thazhe K. Prasad, Melath V. Rajasekharan,* and Jean-Pierre Costes*

Construction and characterization of metal–organic frameworks (MOFs) continue to attract much attention owing to their potential to produce solid-state materials with useful properties. Heterometallic compounds formed from lanthanides and transition-metal ions are of interest because of their magnetic properties,^[1] especially because some of them behave as single-molecule magnets.^[2] Though much work has been done with lanthanides and copper, there are only a few coordination networks with lanthanide(III) and manganese(II) centers.^[3,4] Oxydiacetic acid ($\text{O}(\text{CH}_2\text{CO}_2\text{H})_2$, odaH₂), a multidentate ligand with five coordination sites, forms a number of MOF structures with lanthanides^[5] and transition-metal ions^[6] as well as 3d–4f composites.^[7]

Herein, we report the synthesis, structure, and magnetic properties of $[\{\text{Mn}(\text{H}_2\text{O})_6\}\{\text{MnGd}(\text{oda})_3\}_2] \cdot 6\text{H}_2\text{O}$ (**1**), which is the first cubic gadolinium–manganese 3D MOF with a ferromagnetic interaction. Compound **1** was obtained as colorless cubes by slow evaporation of an aqueous solution containing the metal salts and odaH₂ at pH 6–7.

The crystal structure consists of a novel anionic 3D cubic network formed with $[\text{Gd}(\text{oda})_3]^{3-}$ and Mn^{2+} as building blocks. Gd^{3+} is nine-coordinate with a distorted tricapped trigonal-prismatic geometry formed by the coordination of three oxygen (two carboxylate and one alkoxo) atoms from each oda ligand. The octahedral coordination sphere of Mn^{2+} is formed by six free carboxylate oxygen atoms from six neighboring $[\text{Gd}(\text{oda})_3]^{3-}$ units (Figure 1). $[\text{Gd}(\text{oda})_3]^{3-}$ unit is surrounded by six Mn^{2+} units and vice-versa, creating a cubic lattice with voids in the structure (Figure 2). As shown in Figure 3, the metal-only lattice permits only one type of channel. However the carbon atoms of the oda ligand project into these channels, alternatively narrowing and broadening it, resulting in two types of cavities. The bigger cavity is

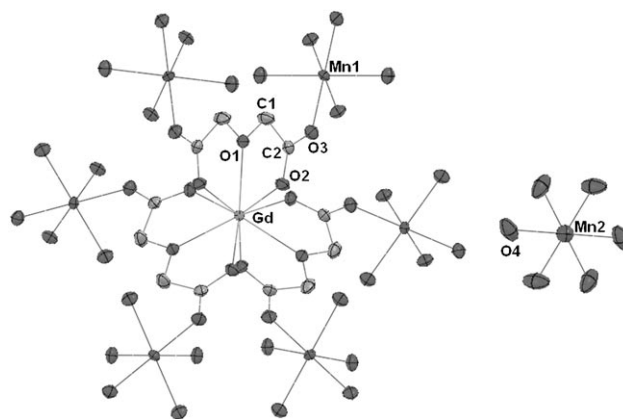


Figure 1. ORTEP diagram of **1**. Thermal ellipsoids are set at 30% probability; H atoms and solvent water molecules are omitted.

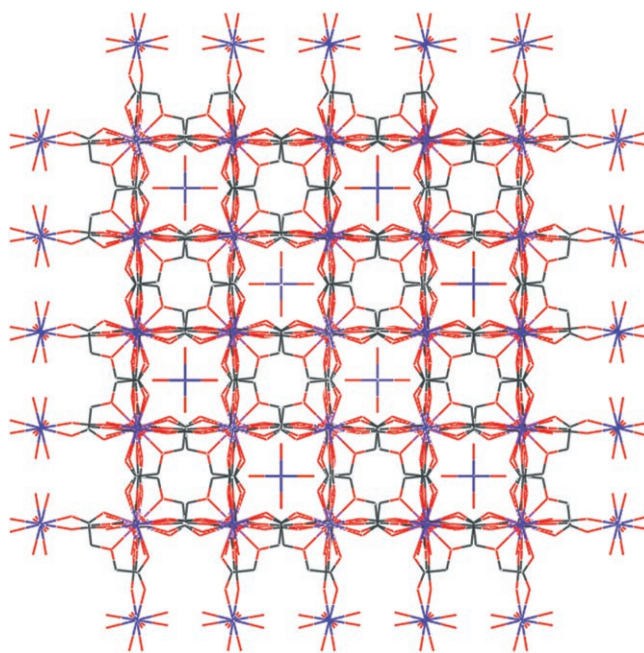


Figure 2. View along an axis of the unit cell of **1** showing the two types of cavities. H atoms and solvent water molecules are omitted. Gd purple, Mn blue, C gray, O red.

occupied by the $[\text{Mn}(\text{H}_2\text{O})_6]^{2+}$ unit, which acts as a counterion to neutralize the charge of the MOF, while the smaller cavity is filled with solvent water molecules which are hydrogen-bonded to the carboxylate oxygen atom of oda. The ability of $[\text{Mn}(\text{H}_2\text{O})_6]^{2+}$ to act as a cation in MOF has been reported.^[8] Even though there are lattice water mole-

[*] T. K. Prasad, Dr. M. V. Rajasekharan
School of Chemistry
University of Hyderabad
Hyderabad – 500046 (India)
Fax: (+91) 40-2301-2460
E-mail: mvrsc@uohyd.ernet.in

Dr. J.-P. Costes
Laboratoire de Chimie de Coordination
205, route de Narbonne, 31077 Toulouse Cedex 4 (France)
Fax: (+33) 5-6155-3003
E-mail: costes@lcc-toulouse.fr

[**] The X-ray data were collected at the diffractometer facility at University of Hyderabad, established by the Department of Science and Technology, Government of India. Infrastructure support from UGC (UPE program) is also acknowledged. This work was supported by CSIR, India. T.K.P. thanks the CSIR for award of a senior research fellowship.

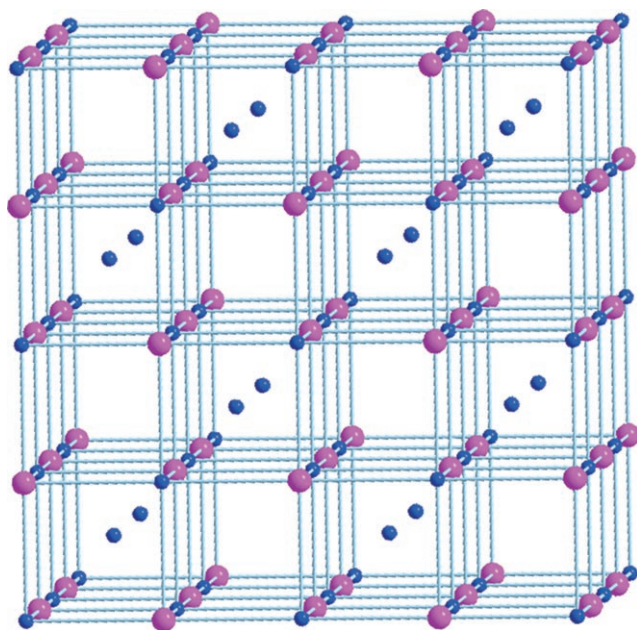


Figure 3. View along an axis of the unit cell of **1** showing the metal centers. Gd purple, Mn blue.

cules situated along the three axes of the Mn^{2+} octahedron, their disposition is not suitable for any significant hydrogen-bonding interaction with the coordinated water molecules. In other words, only the oda oxygen atoms act as hydrogen-bond acceptors for both types of water molecules. A perspective view of the crystal packing is shown in Figure 4. The important bond lengths in the compound are the following: $\text{Gd}-\text{O}_{(\text{carboxylate})}$ 2.370(6), $\text{Gd}-\text{O}_{(\text{alkoxo})}$ 2.429(8), $\text{Mn}-\text{O}_{(\text{carboxylate})}$

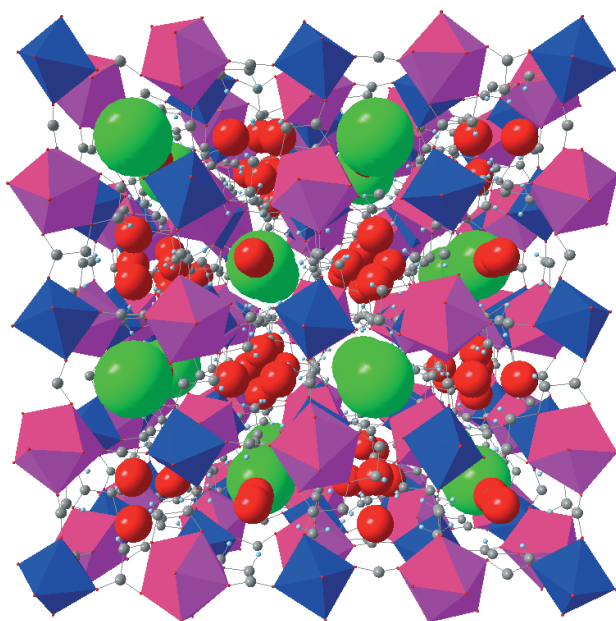


Figure 4. Perspective view along an axis of the unit cell of **1**. Gd and Mn coordination polyhedra in the MOF are shown in purple and blue, respectively. $[\text{Mn}(\text{H}_2\text{O})_6]^{2+}$ ions and solvent water molecules are shown as large green and red spheres, respectively. Gd purple, Mn blue, C gray, O red; H omitted.

2.168(6), and $\text{Mn}-\text{OH}_2$ 2.195(11) Å. The Gd–Mn distance in the MOF is 6.469(1) Å, and the $\text{Gd}-\text{Mn}_{(\text{ion})}$ and $\text{Mn}-\text{Mn}_{(\text{ion})}$ distances are both 5.602(1) Å. It is also noteworthy that the acetate Gd–Mn bridges are in the less common *anti-anti* conformation.^[9]

All the reported 3d–4f MOFs with odaH₂ consist of lanthanide (Ln) and copper or zinc ions crystallizing in a hexagonal lattice with similar structures.^[7] In all cases, the free oxygen of the $[\text{Ln}(\text{oda})_3]^{3-}$ moiety is coordinated to the transition metal. The coordination sphere of the transition metal consists of four carboxylate oxygen atoms from the $[\text{Ln}(\text{oda})_3]^{3-}$ unit and two water molecules coordinated in the axial positions, leading to the formation of $[\text{M}_3\text{Ln}_2(\text{oda})_6(\text{H}_2\text{O})_6]$ ($\text{M} = \text{Cu}, \text{Zn}$), a neutral, porous 3D network structure. Furthermore, the acetate group bridging M and Ln ions is in a *syn-anti* conformation. In the present structure, the main difference comes from the coordination of the manganese unit in the MOF, which, in contrast to the copper or zinc ions described above, is not coordinated by water. Instead, the octahedral coordination is achieved by six carboxylate oxygen atoms of the $[\text{Ln}(\text{oda})_3]^{3-}$ units, resulting in a lattice change from hexagonal to cubic. There are only a few compounds in which water molecules occupy the axial position of the manganese coordination sphere, whereas such coordination is much more common for copper. The relative amounts of the lanthanide, transition metal, and ligand present in both structures are same as in $[\text{Mn}_3\text{Gd}_2(\text{oda})_6(\text{H}_2\text{O})_6]$. The greater preference of Mn^{2+} for regular octahedral coordination over 4 + 2 coordination must be important for the formation of the cubic network. Nevertheless, the Ln–Mn compound $[\text{Mn}_3\text{Ln}_2(\text{dipic})_6(\text{H}_2\text{O})_6]$ (dipicH_2 = pyridine-2,6-dicarboxylic acid) crystallized in a hexagonal lattice with two water molecules occupying the axial positions of the manganese atom.^[3]

Magnetic-susceptibility measurements for **1** have been performed on a Quantum Design MPMS SQUID magnetometer in the 2–300 K temperature range and with an applied field of 1000 Oe. The thermal variation of the product of the molar magnetic susceptibility and the temperature, $\chi_{\text{M}}T$, for the complex **1**, corrected for the diamagnetism of the ligands,^[10] is shown in Figure 5, with the χ_{M} value corresponding to the susceptibility of the pentanuclear entity $[\{\text{Mn}(\text{H}_2\text{O})_6\}[\text{MnGd}(\text{oda})_3]_2] \cdot 6\text{H}_2\text{O}$. At 300 K, $\chi_{\text{M}}T$ is equal to $28.53 \text{ cm}^3 \text{ mol}^{-1} \text{ K}$, which is slightly smaller than expected

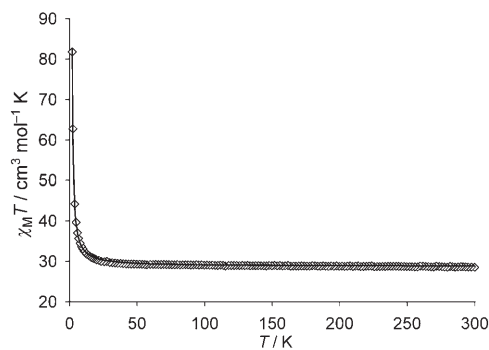


Figure 5. Temperature dependence of $\chi_{\text{M}}T$ for **1** at 0.1 T (◇) compared with the Curie–Weiss best fit (—).

(28.87 cm³mol⁻¹K) for five isolated ions (3Mn²⁺ + 2Gd³⁺). Upon lowering the temperature, $\chi_M T$ first increases slowly until 25 K (29.96 cm³mol⁻¹K) and then increases sharply up to 81.87 cm³mol⁻¹K at 2 K. This behavior confirms the presence of ferromagnetic Mn–Gd interactions in the 3D structure. Surprisingly, the $\chi_M T$ value at 2 K is not far from the value expected for a Gd₂–Mn₂ entity with ferromagnetic interactions ($S=24/2$) and an isolated Mn²⁺ ion (82.37 cm³mol⁻¹K). According to the structural determination that confirms the existence of a 3D cubic network with equal Mn–O and Gd–O bond lengths and angles and the presence of Gd³⁺ and Mn²⁺ ions with their half-filled 4f and 3d orbitals, the six Mn–Gd interaction pathways can be considered identical, giving a highly isotropic system. The mathematical model corresponding to such a structure is not known, but, owing to this high symmetry, a unique interaction parameter $J_{\text{Mn–Gd}}$ is needed. The simplest way to analyze the system is to consider it as obeying the Curie–Weiss law. This fit gives a θ value of 1.304(2) K for a g value of 2.00 (Figure 5). The X-band electron paramagnetic resonance (EPR) spectrum at 4 K gives a large signal centered at $g=2.01$. The positive θ value agrees with a ferromagnetic J interaction. A rough estimate of the interaction parameters can be obtained by considering the system as a tetranuclear species with a unique J parameter. After subtracting the paramagnetic contribution from the [Mn(H₂O)₆]²⁺ ion, the resulting experimental data were fitted to the Hamiltonian $H = -J(S_{\text{Gd1}}S_{\text{Mn1}} + S_{\text{Gd2}}S_{\text{Mn1}} + S_{\text{Gd2}}S_{\text{Mn2}} + S_{\text{Gd1}}S_{\text{Mn2}})$ in which each Mn²⁺ ion interacts with two Gd³⁺ ions and vice-versa. Such a model overestimates the J parameter, because it only takes into account two Gd–Mn interactions instead of the six present in the 3D system. Using exact diagonalization of the tetranuclear unit,^[11] a correct agreement between the experimental and calculated values is found, with $J=0.24$ cm⁻¹, $g=2.0$ (Figure 6). The restricted model cannot fit the data at low temperature, as a consequence of its limited nuclearity. It has the merit of giving the limit of J (0.24 cm⁻¹), a reasonable value being estimated to be equal to or slightly lower than 0.1 cm⁻¹. Recently, it has been suggested that the Mn²⁺ ion with its stable 3d⁵ electronic configuration would not be able to transmit a ferromagnetic Mn–Gd interaction.^[3d] Our example does not support this assertion. The ferromagnetic

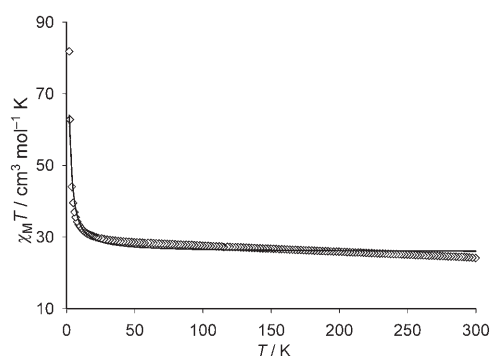


Figure 6. Temperature dependence of $\chi_M T$ for **1** at 0.1 T after subtraction of the paramagnetic contribution of the [Mn(H₂O)₆]²⁺ ions (◇) compared with the best fit obtained for a tetranuclear Gd₂Mn₂ entity (—). See text for details.

behavior must be explained by the *anti-anti* conformation of the acetate bridge. Indeed, the 3d–4f compounds with carboxylate bridges in the *syn-anti* conformation present weak antiferromagnetic interactions.^[3,7] It is also evident that the presence of one unique type of bridge in a very isotropic system facilitates the interaction. Although weak, the ferromagnetic Gd–Mn interaction with $J < 0.24$ cm⁻¹ is further supported by magnetization measurements in the 0–5 T range at 2 K (Figure 7). The experimental values are located between the lines corresponding to uncoupled Gd³⁺ and Mn²⁺ ions and to an $S=24/2$ state plus the contribution of the isolated paramagnetic Mn²⁺ ion.

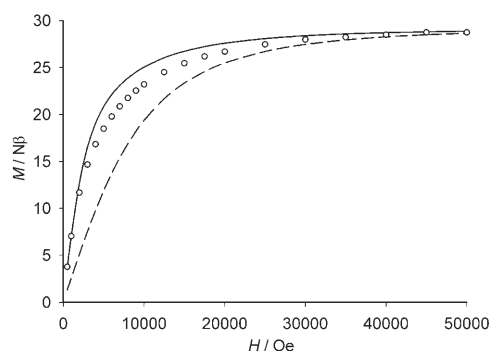


Figure 7. Field dependence of the magnetization of **1** at 2 K (○) compared with the Brillouin function for uncoupled Gd³⁺ and Mn²⁺ ions (----) and the Brillouin function for an $S=24/2$ state plus an $S=5/2$ state (—).

The main goal of this work is to demonstrate for the first time that 3D 3d–4f MOFs with cubic lattices do exist. They may be considered as analogous to the Prussian blue entities observed with 3d ions.^[12] At first sight, this result is a bit surprising, because lanthanide ions need a high coordination number, which makes such an arrangement unfavorable. It is clear that the ligand plays an important role in this case. Indeed, from the nine coordination sites around the Gd³⁺ ion, only six are able to link Mn²⁺ ions through the acetate bridges. As the Mn²⁺ ions are also linked to six different acetate bridges, a 1:1 Gd:Mn ratio is obtained. The charge compensation is achieved by a supplementary Mn²⁺ ion, to give the final [Mn(H₂O)₆]₂[MnGd(oda)₃]₂·6H₂O formulation. In summary, we can affirm that the ligand and the 3d ion have a predominant role in inducing a change from the known hexagonal structures to the novel cubic one. Furthermore the *anti-anti* conformation of the acetate bridge favors the ferromagnetic Gd–Mn interaction. Because of the high isotropy of this system, only one magnetic interaction is needed to describe its magnetic properties, so that the other Mn–Ln complexes in this series can be considered as good candidates for a future and more thorough study of their magnetic properties. Work in this direction is in progress.

Experimental Section

1: An aqueous solution (2 mL) of Gd(NO₃)₃·5H₂O (0.442 g, 1.02 mmol) was added to an aqueous solution (10 mL) of odaH₂

(0.404 g, 3.01 mmol), and the pH value was adjusted to 6.5–7.0 with aqueous ammonia. An aqueous solution (2 mL) of $\text{MnSO}_4 \cdot \text{H}_2\text{O}$ (0.252 g, 1.49 mmol) was subsequently added, the pH value of the solution was readjusted to 6.5–7.0, and the solution was filtered and the filtrate was kept for evaporation at room temperature. After one day, small colorless cubic crystals suitable for X-ray data collection formed, which were removed after two days. Yield: 0.287 g, 19%. Elemental analysis (%) calcd for $\text{C}_{24}\text{H}_{48}\text{Gd}_2\text{Mn}_3\text{O}_{42}$ (1487.94): C 19.37, H 3.25; found: C 19.98, H 2.43. IR (KBr disk): $\tilde{\nu}$ = 3400, 1690, 1541, 1414, 1312, 1122, 1049, 939 cm^{-1} .

X-ray crystal structure determination was performed with a Bruker SMART APEX CCD X-ray diffractometer, using graphite-monochromated $\text{MoK}\alpha$ radiation ($\lambda = 0.71073 \text{ \AA}$). The data was reduced using SAINTPLUS^[13] and a multiscan absorption correction using SADABS^[14] was performed. The structure was solved using SHELXS-97, and full-matrix least-squares refinement against F^2 was carried out using SHELXL-97.^[15] Crystal data for **1**: $\text{C}_{24}\text{H}_{48}\text{Gd}_2\text{Mn}_3\text{O}_{42}$, $M_r = 1487.94$, cubic, $Fd\bar{3}c$, $a = 25.8769(18) \text{ \AA}$, $V = 17328(2) \text{ \AA}^3$, $Z = 16$, $T = 298 \text{ K}$, $\mu = 4.001 \text{ mm}^{-1}$, $\rho_{\text{calcd}} = 2.281 \text{ g cm}^{-3}$, $2\theta_{\text{max}} = 28.65$, reflections collected/independent ($I > 2\sigma(I)$) = 41 294/919, $R_{\text{int}} = 0.0928$, $R(F_o^2) = 0.0508$ ($I > 2\sigma(I)$), $R_w(F_o^2) = 0.1389$ ($I > 2\sigma(I)$), largest difference peak, hole = 1.520, $-1.400 \text{ e \AA}^{-3}$. CCDC 630887 contains the supplementary crystallographic data for this paper. These data can be obtained free of charge from The Cambridge Crystallographic Data Centre via http://www.ccdc.cam.ac.uk/data_request/cif.

Received: December 15, 2006

Published online: March 12, 2007

Keywords: 3d–4f networks · hybrid materials · lanthanides · magnetic properties · manganese

- [1] C. Benelli, D. Gatteschi, *Chem. Rev.* **2002**, *102*, 2369–2387.
- [2] a) J.-P. Costes, F. Dahan, W. Wernsdorfer, *Inorg. Chem.* **2006**, *45*, 5–7; b) C. Aronica, G. Pilet, G. Chastanet, W. Wernsdorfer, J.-F. Jacquot, D. Luneau, *Angew. Chem.* **2006**, *118*, 4775–4778; *Angew. Chem. Int. Ed.* **2006**, *45*, 4659–4662; c) M. Ferbinteanu, T. Kajiwar, K.-Y. Choi, H. Nojiri, A. Nakamoto, N. Kojima, F. Cimpoesu, Y. Fujimura, S. Takaishi, M. Yamashita, *J. Am. Chem. Soc.* **2006**, *128*, 9008–9009; d) A. Mishra, W. Wernsdorfer, K. A. Abboud, G. Christou, *J. Am. Chem. Soc.* **2004**, *126*, 15648–15649; e) S. Osa, T. Kido, N. Matsumoto, N. Re, A. Pochaba, J. Mrozinski, *J. Am. Chem. Soc.* **2004**, *126*, 420–421; f) C. M. Zaleski, E. C. Depperman, J. W. Kampf, M. L. Kirk, V. L. Pecoraro, *Angew. Chem.* **2004**, *116*, 4002–4004; *Angew. Chem. Int. Ed.* **2004**, *43*, 3912–3914.
- [3] a) B. Zhao, H. Gao, X. Chen, P. Cheng, W. Shi, D. Liao, S. Yan, Z. Jiang, *Chem. Eur. J.* **2006**, *12*, 149–158; b) B. Zhao, X. Chen, P. Cheng, L. Liao, S. Yan, Z. Jiang, *J. Am. Chem. Soc.* **2004**, *126*, 15394–15395; c) B. Zhao, P. Cheng, X. Chen, C. Cheng, W. Shi, D. Liao, S. Yan, Z. Jiang, *J. Am. Chem. Soc.* **2004**, *126*, 3012–3013; d) B. Zhao, P. Cheng, Y. Dai, C. Cheng, D. Z. Liao, S. P. Yan, Z. H. Jiang, G. L. Wang, *Angew. Chem.* **2003**, *115*, 964–966; *Angew. Chem. Int. Ed.* **2003**, *42*, 934–936.
- [4] a) Y. Kim, Y. Park, D.-Y. Jung, *Dalton Trans.* **2005**, 2603–2609; b) T. Yi, G. Gao, B. Li, *Polyhedron* **1998**, *17*, 2243–2248; c) T.-Z. Jin, S.-F. Zhao, G.-X. Xu, Y.-Z. Han, N.-C. Shi, Z.-S. Ma, *Acta Chim. Sin. (Chin. Ed.)* **1991**, *49*, 569–575.
- [5] a) T. Behrsing, G. B. Deacon, C. M. Forsyth, M. Forsyth, B. W. Skelton, A. H. White, *Z. Anorg. Allg. Chem.* **2003**, *629*, 35–44; b) R. Baggio, M. Perec, M. T. Garland, *Acta Crystallogr., Sect. C* **2000**, *56*, 312–315; c) P. F. Aramendia, R. Baggio, M. T. Garland, M. Perec, *Inorg. Chim. Acta* **2000**, *303*, 306–310; d) R. Baggio, M. T. Garland, M. Perec, *Acta Crystallogr. Sect. C* **1998**, *54*, 591–594; e) R. Baggio, M. T. Garland, M. Perec, *Inorg. Chim. Acta* **1998**, *281*, 18–24; f) R. Baggio, M. T. Garland, M. Perec, D. Vega, *Inorg. Chem.* **1996**, *35*, 2396–2399.
- [6] a) A. Grirrane, A. Pastor, E. Alvarez, C. Mealli, A. Ienco, P. Rosa, F. Montilla, A. Galindo, *Eur. J. Inorg. Chem.* **2004**, 707–717; b) P. M. Forster, A. K. Cheetham, *Microporous Mesoporous Mater.* **2004**, *73*, 57–64; c) A. Grirrane, A. Pastor, C. Mealli, A. Ienco, P. Rosa, R. Prado-Gotor, A. Galindo, *Inorg. Chim. Acta* **2004**, *357*, 4215–4219; d) C. Jiang, Z.-Y. Wang, *Polyhedron* **2003**, *22*, 2953–2959; e) C. Jiang, X. Zhu, Z.-P. Yu, Z.-Y. Wang, *Inorg. Chem. Commun.* **2003**, *6*, 706–709.
- [7] a) A. C. Rizzi, R. Calvo, R. Baggio, M. T. Garland, O. Pena, M. Perec, *Inorg. Chem.* **2002**, *41*, 5609–5614; b) R. Baggio, M. T. Garland, Y. Moreno, O. Pena, M. Perec, E. Spodine, *J. Chem. Soc. Dalton Trans.* **2000**, 2061–2066; c) R. Baggio, M. Perec, M. T. Garland, *Acta Crystallogr., Sect. C* **2003**, *59*, m175–m177; d) B. Barja, R. Baggio, M. T. Garland, P. F. Aramendia, O. Pena, M. Perec, *Inorg. Chim. Acta* **2003**, *346*, 187–196; e) Q.-D. Liu, J.-R. Li, S. Gao, B.-Q. Ma, F.-H. Liao, Q.-Z. Zhou, K.-B. Yu, *Inorg. Chem. Commun.* **2001**, *4*, 301–304; f) J. Torres, F. Peluffo, S. Dominguez, A. Mederos, J. M. Arrieta, J. Castiglioni, F. Lloret, C. Kremer, *J. Mol. Struct.* **2006**, *825*, 60–69.
- [8] a) B. O. Patrick, C. L. Stevens, A. Storr, R. C. Thompson, *Polyhedron* **2003**, *22*, 3025–3035; b) L. P. Wu, M. Yamamoto, T. Kuroda-Sowa, M. Maekawa, J. Fukui, M. Munakata, *Inorg. Chim. Acta* **1995**, *239*, 165–169.
- [9] a) E. Colacio, J. M. Dominguez-Vera, R. Kivekäs, J. M. Moreno, A. Romerosa, J. Ruiz, *Inorg. Chim. Acta* **1993**, *212*, 115–121; b) E. Colacio, J. M. Dominguez-Vera, M. Ghazi, R. Kivekäs, M. Klinga, J. M. Moreno, *Eur. J. Inorg. Chem.* **1999**, 441–445.
- [10] P. Pascal, *Ann. Chim. Phys.* **1910**, *19*, 5.
- [11] a) J. J. Borrás-Almenar, J. M. Clemente-Juan, E. Coronado, B. S. Tsukerblat, *Inorg. Chem.* **1999**, *38*, 6081–6088; b) J. J. Borrás-Almenar, J. M. Clemente-Juan, E. Coronado, B. S. Tsukerblat, *J. Comput. Chem.* **2001**, *22*, 985–991; c) MINUIT Program, a System for Function Minimization and Analysis of the Parameters Errors and Correlations: F. James, M. Roos, *Comput. Phys. Commun.* **1975**, *10*, 345.
- [12] M. Verdager, A. Bleuzen, V. Marvaud, J. Vaissermann, M. Seuleiman, C. Desplanches, A. Scullier, C. Train, R. Garde, G. Gelly, C. Lomenech, I. Rosenman, P. Veillet, C. Cartier, F. Villain, *Coord. Chem. Rev.* **1999**, *190–192*, 1023–1047.
- [13] SAINTPLUS, Bruker AXS Inc., Madison, (USA) **2003**.
- [14] G. M. Sheldrick, SADABS, Program for Empirical Absorption Correction, University of Göttingen (Germany) **1996**.
- [15] G. M. Sheldrick, SHELX-97, Programs for Crystal Structure Analysis, University of Göttingen (Germany) **1997**.